## PAPER

Check for updates

# Knots modify the coil–stretch transition in linear DNA polymers†

Beatrice W. Soh, [a] Vivek Narsimhan, [b] Alexander R. Klotz [a] and Patrick S. Doyle *[a]

We perform single-molecule DNA experiments to investigate the relaxation dynamics of knotted polymers and examine the steady-state behavior of knotted polymers in elongational fields. The occurrence of a knot reduces the relaxation time of a molecule and leads to a shift in the molecule's coil–stretch transition to larger strain rates. We measure chain extension and extension fluctuations as a function of strain rate for unknotted and knotted molecules. The curves for knotted molecules can be collapsed onto the unknotted curves by defining an effective Weissenberg number based on the measured knotted relaxation time in the low extension regime, or a relaxation time based on Rouse/Zimm scaling theories in the high extension regime. Because a knot reduces a molecule's relaxation time, we observe that knot untying near the coil–stretch transition can result in dramatic changes in the molecule's conformation. For example, a knotted molecule at a given strain rate can experience a stretch–coil transition, followed by a coil–stretch transition, after the knot partially or fully unties.

## 1 Introduction

Developments in microfabrication techniques and fluorescence microscopy over the past few decades have provided a platform for the direct observation and precise manipulation of individual DNA molecules. Single-molecule experiments have been widely used to investigate the static and dynamic properties of DNA as a model polymer.[1] Such studies not only serve to address fundamental questions in polymer physics that cannot be easily accessed *via* bulk methods, but also facilitate the development of emerging DNA mapping and sequencing techniques.[2,3] Studies on the dynamics of individual molecules subjected to model flows and fields have been enabled by the fabrication of various microfluidic device geometries, such as parallel plates,[4] hyperbolic contractions,[5,6] T-junctions,[7] and cross-slot channels.[8–13] Most notably, the stretching of individual DNA molecules in elongational flows showed that molecules unraveling in flow exhibit heterogeneous stretching dynamics that are largely dependent on the initial molecular conformation[8,9] – a behavior termed molecular individualism[14] – and also demonstrated the existence of coil–stretch hysteresis in long DNA molecules.[10] Most experiments to date have involved

linear DNA molecules,[15] although there is recent interest in circular DNA molecules,[16,17] as well as other complex topologies, including molecules with branches[18] and knots.[19,20]

Theoretically, it has been proven that the knotting probability of a chain approaches unity as the chain length tends to infinity, hence knots are inevitably present in long polymer chains.[21] The probability of knot formation in DNA has been studied both computationally[22–24] and experimentally[25,26] on length scales of relevance. Indeed, knots are known to occur in DNA,[27,28] proteins[29,30] and synthetic polymers.[31] The presence of knots is known to have important ramifications for biology and biotechnology applications, from adding complexities to the folding energy landscapes of proteins[32] to halting translocation of polymers through nanopores.[33,34] From the perspective of polymer physics, knots have also been shown to affect overall polymer properties.[19,35–39] For example, simulations have indicated that a knot reduces the mechanical strength of a polymer chain, and that a knotted chain under tension almost always breaks at the entrance to the knot.[35]

Most studies on knotted polymers to date have been theoretical and computational in nature.[35–40] Over the past decade, researchers have demonstrated experimental methods of introducing knots in biopolymers *via* chemical synthesis,[41,42] optical tweezers[43,44] and electric fields.[45,46] The development of such techniques has ignited interest in the experimental probing of knotted polymer dynamics. Knots tied onto DNA chains held under tension were found to be mobile, and the diffusion of different knot types was observed and quantified.[44] Previous work from our group investigated the swelling of knots in DNA molecules during chain relaxation and showed that the

[a] *Department of Chemical Engineering, Massachusetts Institute of Technology, Cambridge, Massachusetts 02139, USA. E-mail: pdoyle@mit.edu*

[b] *Department of Chemical Engineering, Purdue University, West Lafayette, Indiana 47907, USA*

† Electronic supplementary information (ESI) available: Additional details regarding knot size measurements and analysis, estimate of maximum knotted molecule extension, additional extension-Wi and standard deviation plots, calculation of confidence intervals, and movies. See DOI: 10.1039/c7sm02195j

knot growth time scale is governed by the global chain relaxation time scale.[20] Knotted DNA molecules subjected to elongational fields were shown to exhibit nucleation-type behavior of the coil–stretch transition and to stretch at a much slower rate compared to unknotted molecules.[19] Experimentally, the dynamics of knotted polymers is a rich area for exploration. In particular, the effect of knots on the relaxation dynamics of polymers has yet to be investigated experimentally in detail.

Recently, our group performed a computational study of the steady-state and transient dynamics of knotted polymers in elongational flow and examined how knots modify the relaxation time of a chain.[40] In the present work, we use single-molecule experiments to study the relaxation dynamics of knotted polymers and the effects of a knot on steady-state behavior of polymer chains in elongational fields. We use strong electric fields to induce knots in DNA molecules *via* an electrohydrodynamic instability[45] and quantify the relaxation times of knotted molecules in relation to knot size. We then subject molecules with knots to planar elongational fields and observe the steady-state dynamics of the chain. Specifically, we focus on the steady-state fractional extension and extension fluctuations of the chain, and compare the dynamics of molecules with and without a knot. We find that the occurrence of a knot markedly changes the steady-state chain dynamics in elongational fields, which can be resolved by taking into account the faster relaxation time and reduction in free chain contour of the knotted molecule.

## 2 Experimental methods

### 2.1 Channel and DNA preparation

A charged molecule with electrophoretic mobility $\mu$ in an electric field of magnitude $E$ moves with a velocity $v = \mu E$.

The kinematics of a planar elongational electric field can be described by considering the velocity of charged molecules in the field:

$$v_x = \mu E_x = \dot{\varepsilon}x \qquad (1)$$

$$v_y = \mu E_y = -\dot{\varepsilon}y \qquad (2)$$

where $v_x$ and $v_y$ are the velocities in the $x$ and $y$ directions respectively, $E_x$ and $E_y$ are the electric fields in the $x$ and $y$ directions respectively, and $\dot{\varepsilon}$ is the strain rate. Electric fields are useful for generating elongational fields because the field kinematics are purely elongational on length scales larger than the Debye length and shear components near surfaces are negligible.[47] Previous studies have used cross-slot channels with hyperbolically curved sidewalls to generate homogeneous elongational electric fields.[13,19,48,49] In this study, we utilized 2.5 μm tall cross-slot channels constructed in polydimethylsiloxane (PDMS, Sylgard 184, Dow Corning) using soft lithography on a silicon master template (SU8-2 photoresist). The channels were soaked overnight in 0.5× Tris–boric acid–EDTA (TBE, AccuGENE) to eliminate permeation-driven flow,[50] rinsed quickly with water and dried with argon, then sealed to a clean glass cover slide. Prior to exposure to DNA molecules, the channels were flushed with experimental buffer by applying a moderate electric field of ∼20 V cm⁻¹ for at least 30 minutes. Independently applied potentials to side reservoirs of the cross-slot channel enabled control over the location of the stagnation point and trapping of molecules at the stagnation point for long times. The strain rate was calibrated against applied voltage as described in previous studies[13,19] and varied by changing the applied voltage at the side reservoirs.

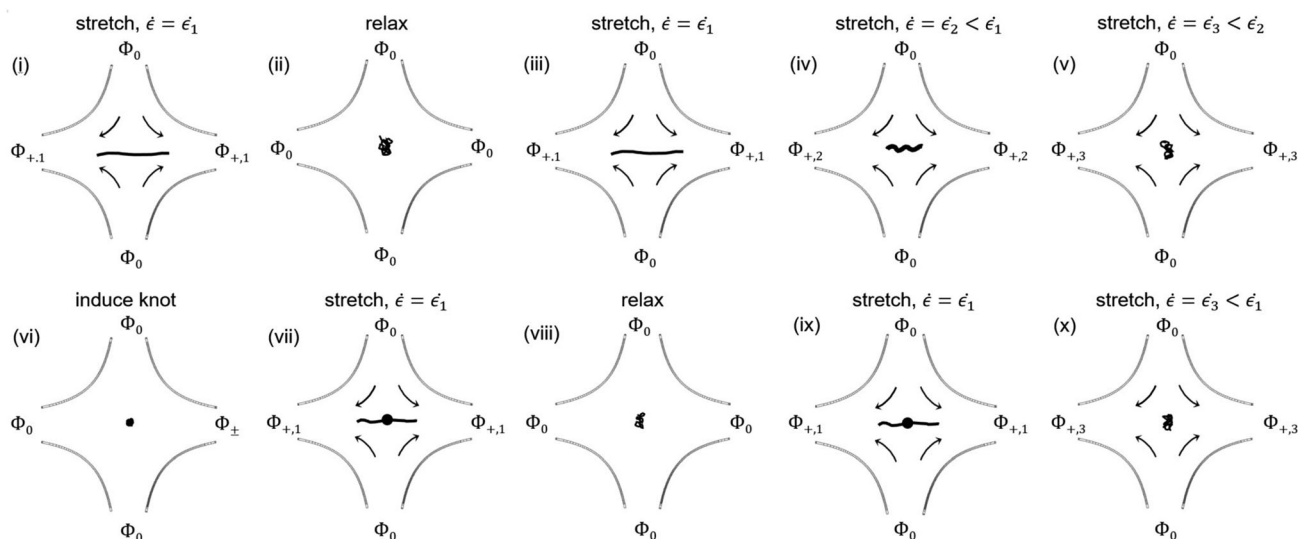The experimental buffer contained 4 vol% β-mercaptoethanol (BME, Calbiochem) and 0.1% 10 kDa polyvinylpyrrolidone



**Fig. 1** Schematic for experimental procedure. (i) A molecule was stretched at the stagnation point of a planar elongational field with strain rate $\dot{\varepsilon} = \dot{\varepsilon}_1$. (ii) The field was turned off and the molecule was allowed to relax back to equilibrium. (iii) The molecule was stretched at strain rate $\dot{\varepsilon} = \dot{\varepsilon}_1$. (iv and v) The strain rate was progressively lowered until the molecule underwent the stretch–coil transition. (vi) A square-wave electric field of strength $E_{rms} \sim 1500$ V cm⁻¹ and frequency f = 10 Hz was turned on for <1 s to compress and induce a knot in the molecule. (vii and viii) The knotted molecule was stretched at strain rate $\dot{\varepsilon} = \dot{\varepsilon}_1$. The field was then turned off and the molecule was allowed to relax back to equilibrium. (ix and x) The knotted molecule was stretched at strain rate $\dot{\varepsilon} = \dot{\varepsilon}_1$ and at progressively lower strain rates until it underwent the stretch–coil transition.

(PVP, Polysciences) in 0.5× TBE solution. T4 DNA (165.6 kbp, Nippon Gene) was stained with fluorescent dye YOYO-1 (Invitrogen) at a base pair to dye ratio of 4 : 1, resulting in a 38% increase in DNA contour length[51] and a stained contour length of 77 μm. The stained DNA solution was allowed to sit at least 12 hours prior to use and diluted in experimental buffer to an optimal viewing concentration of 0.03 μg mL$^{-1}$ immediately before experiments. Single DNA molecules were observed using an inverted Zeiss Axiovert microscope with a 63× 1.4 NA oil-immersed objective and images were recorded using a Photometrics Prime 95B sCMOS camera. The extension of the molecule $X_{ex}$ was determined by the projected distance along the primary axis of extension of the field.

## 2.2 Experimental procedure

The experimental procedure for measuring relaxation times and stretching unknotted and knotted DNA molecules at different strain rates is summarized in Fig. 1. A given T4 DNA molecule was stretched to high extension at the stagnation point in a strong elongational field. The field was then switched off and the relaxation of the molecule back to equilibrium was observed. After allowing the molecule to relax at equilibrium for ~10 s, the field was switched on and the molecule was stretched at a high strain rate. The strain rate was lowered progressively until the molecule transitioned from a stretched to coiled state. The molecule was observed at each strain rate for at least 2 minutes. A knot was then induced in the molecule by applying an AC square-wave electric field of strength $E_{rms}$ ~ 1500 V cm$^{-1}$ and frequency $f$ = 10 Hz for <1 s.[45] The knotted molecule was stretched to high extension in a strong elongational field. The field was then switched off and the relaxation of the molecule back to equilibrium was observed. The field was switched on and the knotted molecule was stretched at a high strain rate. As with the unknotted molecule, the strain rate was stepped downward until the molecule underwent the stretch–coil transition. The knotted molecule was observed at each strain rate for at least 2 minutes. Multiple stretch–relax cycles were performed for each unknotted and knotted molecule. Knotted molecules were limited to remain in the coiled state for no more than ~5 relaxation times between stretch–relax cycles to minimize partial knot untying over multiple relaxations. Steady-state configurations of molecules were analyzed only after the molecule had experienced a certain strain rate for ~5 s.

## 2.3 Relaxation time measurements

During each relaxation process, the extension of a given molecule $X_{ex}$ as a function of time was recorded. To extract a longest relaxation time that is consistent with rheological stress relaxation measurements,[15] we fit the last 30% of extension that corresponds to the linear force regime of the spring force law to a single-exponential decay according to the equation

$$\langle X_{ex}{}^2 \rangle = \langle X_{ex,eq}{}^2 \rangle + \left( \langle X_{ex,0}{}^2 \rangle - \langle X_{ex,eq}{}^2 \rangle \right) \exp\left( \frac{-t}{\tau} \right) \quad (3)$$

where $X_{ex}$ is the extension of the molecule, $X_{ex,0}$ is the extension of the molecule at the start of the fitting region and $t$ is time.

The equilibrium extension $X_{ex,eq}$ and longest relaxation time $\tau$ are fitted parameters. As knots along a linear chain exist in a metastable topological state,[52,53] the equilibrium extension $X_{ex,eq}$ for a knotted molecule refers to the extension of the molecule over time scales longer than the relaxation time, but shorter than the time for the knot to diffuse off the chain.

## 2.4 Knot size measurements

In a stretched state, a knotted molecule contains a bright spot that represents a region of excess fluorescence, consistent with the higher density of dye molecules within the knot. While the length scale of the knot is too small to be resolved by fluorescence microscopy, we can use intensity as a measure of the contour length stored within the knot.[20] We use as a measure of fractional knot size the integrated intensity of the knotted region divided by the integrated intensity of the molecule, where the knotted region is defined as a 9-pixel (1.6 μm) window centered around the brightest pixel of the knot. While this is not a direct measure of the knot contour, we find it the most systematic way of characterizing knot sizes for the purposes of this work, as discussed in the ESI.† We emphasize that this method likely leads to an overestimate of the actual knot size, due to the high density of fluorophores within a diffraction-limited spot that is defined as the knotted region.

# 3 Results and discussion

## 3.1 Relaxation dynamics of unknotted and knotted molecules

A series of time lapse images showing the relaxation process for the same molecule without a knot and with a knot is displayed in Fig. 2. At a strain rate $\dot{\varepsilon}$ = 1.3 s$^{-1}$, the molecules are in a highly extended state. After the field is switched off, the extension of the molecules decreases sharply as entropic restoring forces return the molecules to the coiled state. Two stark differences are apparent between the relaxation processes for the unknotted
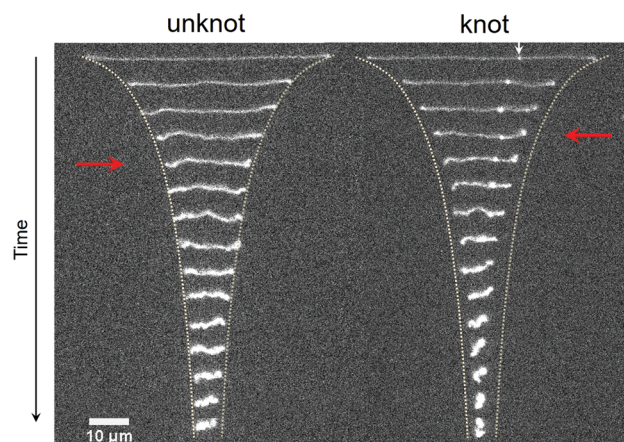


Fig. 2 Time lapse images showing the relaxation of a molecule without a knot (left) and with a knot (right) after switching off the elongational field at strain rate $\dot{\varepsilon}$ = 1.3 s$^{-1}$. The dotted lines are traces of the unknotted relaxation to facilitate comparison. The white arrow indicates the presence of a knot along the chain and the red arrows point to the molecule at ~30% unknotted chain extension. Images taken 0.57 s apart.

and knotted molecules. Firstly, the initial extension of the unknotted molecule is greater than that of the knotted molecule, which arises from contour stored within the knot. Secondly, the molecule containing a knot undergoes a faster relaxation process compared to the molecule without, and reaches the coiled state more quickly. The quicker relaxation of knotted molecules has also been noted qualitatively by Renner *et al.*[19] See the ESI† for movies of an unknotted and knotted molecule relaxing.

We consider the relaxations of an initially unknotted molecule that was induced to contain two knots, one of which eventually untied to leave the molecule with only one knot. Fig. 3 shows the scaled squared extension of the molecule with different number of knots as a function of time. The fractional knot sizes of the single and double knot at $\sim 30\%$ chain extension are $0.07 \pm 0.02$ (95% confidence interval) and $0.16 \pm 0.02$ respectively. Each curve represents the average of three to four relaxations and the dotted lines are the fits to the last 30% extension. Based on the relaxation trajectories, it is evident that the relaxation process depends on the number of knots in the molecule. Specifically, the more knots the molecule has, the quicker the molecule relaxes back to equilibrium. The relaxation times of a molecule containing no knot, one knot and two knots are $1.46 \pm 0.03$ s, $1.28 \pm 0.02$ s and $1.07 \pm 0.02$ s respectively. We observe from the inset of Fig. 3 that the molecule containing two knots has a markedly smaller chain extension at equilibrium compared to the molecule with one knot, which in turn has a smaller chain extension compared to the molecule with no knot, consistent with there being more stored contour in two knots *versus* one knot, and one knot compared to no knot.

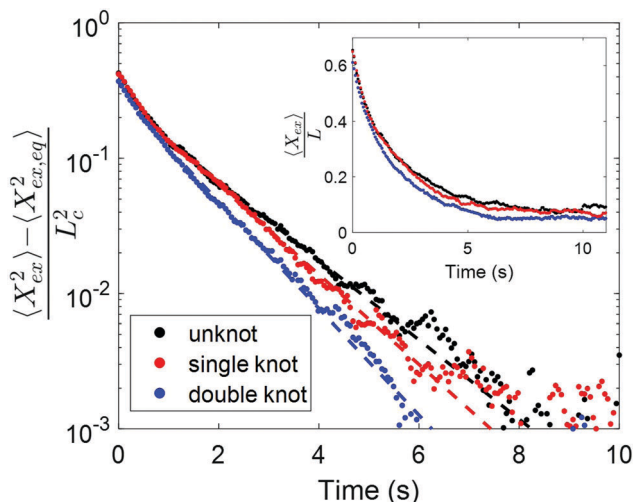Qualitatively, we can rationalize the faster relaxation of knotted molecules by considering the free contour length of the molecule. Previous studies involving knots in T4 DNA molecules induced by an electrohydrodynamic collapse have estimated the knot contour in tight knots to be between 1 μm and 5 μm,[19,20] which corresponds to between 1% and 6% of the contour length. Stored contour in the knot results in the molecule having less free chain contour for relaxation, and smaller molecules relax at a faster rate.[54]

To further investigate the relaxation dynamics of knotted molecules, we quantify the relaxation process for an ensemble of molecules containing knots with a range of sizes. Fig. 4 shows the relaxation times of 24 knotted molecules relative to the relaxation time of unknotted molecules as a function of knot size at $\sim 30\%$ chain extension. Each data point is obtained by averaging over at least four relaxations for the same knotted molecule. Although partial untying of the knot between stretch–relax cycles was possible, we do not observe any discernible trend in knot size over $> 10$ relaxations (see ESI†). The relaxation time of unknotted molecules $\tau_{\text{unknot}}$ is extracted from the relaxation trajectory averaged over 50 relaxations from 24 molecules and determined to be $1.55 \pm 0.02$ s. The knot size for each knotted molecule is measured when the molecule is at $\sim 30\%$ extension, corresponding to the onset of the linear force regime over which the relaxation is fit. It is important to highlight that the knot size continually increases during the relaxation process, thus the reported knot size is not an invariant. As seen from Fig. 4, there is a distinct relationship between relaxation time of a knotted molecule and knot size. In general, the larger the knot size at the onset of the linear force regime, the smaller the relaxation time of the molecule, with a Pearson correlation coefficient of $-0.77$.
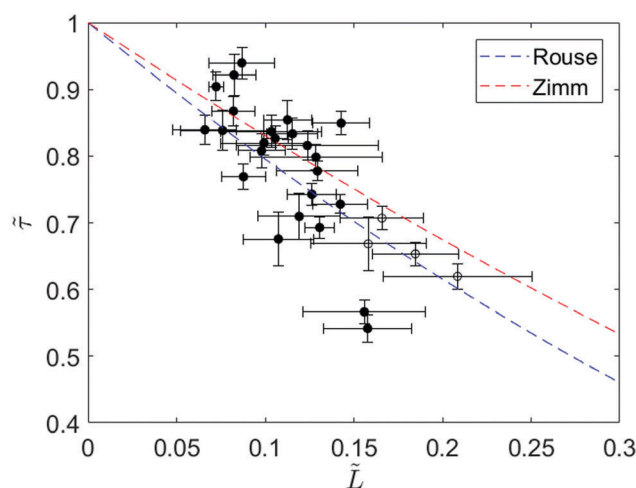


**Fig. 3** Normalized extension as a function of time during relaxation for the same molecule with no knots, one knot (fractional knot size at $\sim 30\%$ extension = $0.07 \pm 0.02$) and two knots (total fractional knot size = $0.16 \pm 0.02$). Each curve represents the average of three to four relaxations. The dotted lines are fits to the data. Inset: Fractional extension as a function of time.



**Fig. 4** Ratio of relaxation times between a knotted and unknotted chain ($\tilde{\tau} = \tau_{\text{knot}}/\tau_{\text{unknot}}$) as a function of fractional knot size at $\sim 30\%$ extension ($\tilde{L} = L_{\text{knot}}/L_{\text{chain}}$) for 24 T4 DNA molecules. Each data point corresponds to a different knotted T4 molecule, averaged over at least four relaxations. The filled circles represent molecules with one knot and the open circles represent molecules with two knots. The fractional knot size is measured as the fraction of chain occupied by the knot at the onset of the linear force regime. The curves correspond to Rouse theory $\tilde{\tau} = (1 - \tilde{L})^{1+2\nu}$ and Zimm theory $\tilde{\tau} = (1 - \tilde{L})^{3\nu}$ where $\nu = 0.588$ is the excluded volume Flory exponent.[55] Error bars represent 95% confidence interval (see ESI† for calculation).

We can understand the faster relaxation times of knotted molecules by considering how the occurrence of knots reduces the free contour length of the chain. According to the Rouse model,[56] the relaxation time of a freely-draining chain scales with chain length as $\tau_{\text{rouse}} \propto L^{1+2\nu}$, where $L$ is the contour length and $\nu = 0.588$ is the excluded volume Flory exponent.[55] For a knotted molecule, the free chain contour that is allowed to relax is $L_{\text{free}} = L_{\text{chain}} - L_{\text{knot}}$. Hence, we have

$$\tau_{\text{rouse}} \propto \left(L_{\text{chain}} - L_{\text{knot}}\right)^{1+2\nu}$$

The Zimm model takes hydrodynamic interactions into account[57] and predicts that the relaxation time of a non-draining chain scales with chain length as $\tau_{\text{rouse}} \propto L^{3\nu}$, thus giving us

$$\tau_{\text{zimm}} \propto \left(L_{\text{chain}} - L_{\text{knot}}\right)^{3\nu}$$

We plot in Fig. 4 the predictions of relaxation time as a function of knot size based on the Rouse and Zimm models. Given the channel height of 2.5 μm used for this study and T4 equilibrium radius of gyration of 1.46 μm,[58] we expect the dynamics to exhibit more Zimm-like behavior.[59] Regardless, for the range of knot sizes considered, the Rouse and Zimm scalings produce similar trends. While the decrease in relaxation time with knot size is generally captured by the Rouse and Zimm scalings, we emphasize that the knot size is not an invariant. As the chain relaxes, the knot continues to grow larger, resulting in progressively less free chain contour. Therefore, the relaxation of a knotted molecule is not equivalent to the relaxation of an unknotted molecule with a fixed, reduced contour length, but instead representative of the relaxation of a molecule with continually decreasing contour length. The varying knot size during the relaxation process is also believed to cause the spread in relaxation times for a given knot size observed in Fig. 4. With some knotted molecules having almost half the relaxation time of unknotted molecules, the demonstrated range of knotted relaxation times reflects the importance of recognizing the reduced free chain contour of a knotted polymer, and suggests that the presence of knots can affect perceived polydispersity of a polymer sample.

Having observed a decrease in relaxation time with increasing knot size, we proceed to consider the effect of knot position on the relaxation process. We look at two molecules with similar knot sizes at ∼30% chain extension. Each molecule experienced 10 stretch–relax cycles, and the fractional knot sizes at ∼30% extension were between 0.12 and 0.14 across all relaxations. While the knot sizes remained largely constant, the knot positions varied through the stretch–relax cycles, with the knots being located at positions spanning about 20% of the chain for each molecule. Due to the difficulty in measuring an accurate knot position on a weakly extended chain, we quantify the knot position in the highly stretched chain prior to switching off the electric field. The knot position is measured as the fractional distance between the center of the knot and closer end of the chain, such that a knot position of 0.35 indicates a knot located 35% into the chain from one end and 65% into the chain from the other end. Although the initial knot position is not necessarily the position of the knot as the chain relaxes, we
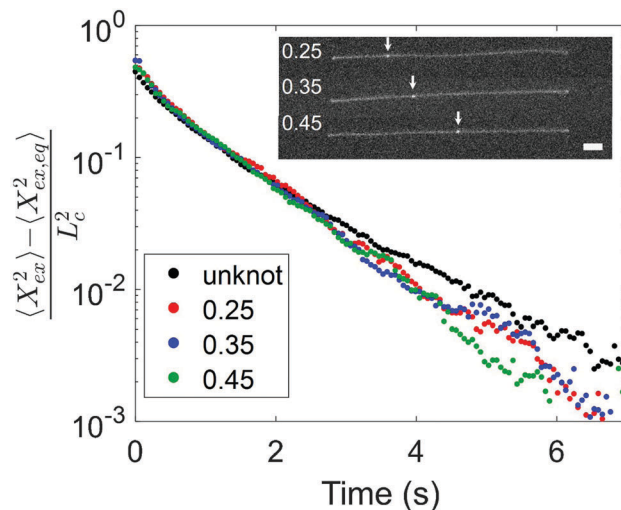


Fig. 5 Normalized extension as a function of time during relaxation for knotted molecules with similar knot sizes but different initial knot positions. Each curve represents the average of between three and five relaxations. All molecules have fractional knot sizes between 0.12 and 0.14 at ∼30% extension. The initial knot position is measured as the fractional length between knot center and closer chain end, and is reported as the fractional position along the chain. An ensemble average relaxation trajectory for unknotted molecules is shown for comparison. Inset: Representative images of molecules with different initial knot positions. The white arrows indicate the locations of the knot along the chain. Scale bar represents 5 microns.

notice that the knot position shifts gradually ($<0.05$) between consecutive relaxations, hence the initial knot position is a reasonable estimate of the knot position during chain relaxation. Fig. 5 shows the averaged trajectories for relaxations of the molecules with different initial knot positions between 0.25 and 0.45. Each curve represents the average of between three and five relaxations. It is evident that the knotted relaxation trajectories are distinct from the unknotted relaxation trajectory. Between the relaxation trajectories of knotted molecules with different knot positions, however, there is no apparent trend. The measured relaxation times are $1.07 \pm 0.03$ s, $1.11 \pm 0.02$ s and $1.05 \pm 0.03$ s for molecules with an initial knot position of 0.25, 0.35 and 0.45 respectively.

We believe that the absent effect of knot position on relaxation time is largely due to the small knot sizes involved. As a knot can effectively be viewed as a bead along the chain with a larger drag coefficient, one would expect that the position of a large enough knot would play a role in determining how the free ends of the chain retract during relaxation. For example, consider the two extreme cases of a knot located in the center of a chain and a knot located near a chain end. The knot near the end of the chain can be seen as an effective tether, which would lead to a different relaxation process compared to the chain with a knot in the center. The sizes of knots generated in this study are likely not large enough for any such effect to be detected.

## 3.2 Steady-state dynamics in elongational fields

The deformation of polymer molecules in elongational flows or fields is a balance between the hydrodynamic drag force exerted

by the flow or field and the entropic force that causes the chain to recoil. The response of molecules in elongational flows and fields is typically characterized by the Weissenberg number Wi, defined as the product of the strain rate and longest relaxation time of the polymer molecule. In this paper, Wi is defined relative to the unknot relaxation time,

$$\text{Wi} \equiv \dot{\varepsilon}\tau_{\text{unknot}}. \tag{4}$$

A coil–stretch transition in elongational flows and fields has been theoretically predicted[60,61] and experimentally observed to occur at Wi ≈ 0.5.[8,9,48] As a knot reduces the relaxation time of a molecule and, consequently, changes the effective Wi characterizing polymer behavior, we are interested in studying the steady-state behavior of knotted polymers in elongational fields.

Fig. 6 displays images of a molecule without and with a knot stretched in planar elongational fields at a range of strain rates. At Wi > 2.0, there are small differences in the extensions of the unknotted and knotted molecules attributable to contour stored within the knot. At moderate Wi, apparent differences in the extensions of the unknotted and knotted molecules emerge, with the knotted molecules exhibiting noticeably smaller extensions at the same Wi. For Wi < 1.0, we observe stark differences in the configurations exhibited by the molecules. Specifically, the knotted molecule has retracted to a coiled state at Wi = 0.7, while the unknotted molecule remains in a stretched state. Evidently, the occurrence of a knot on a molecule reduces the chain relaxation time and consequently shifts the coil–stretch transition. This was also observed computationally in a recent study by Narsimhan *et al.*[40] for a range of knot topologies.

The steady-state extension of unknotted and five different knotted molecules as a function of Wi is plotted in Fig. 7a. The steady-state extension is averaged over an ensemble of 10 molecules for the unknotted molecule and averaged over 30 s to 1 minute ($\sim 30$–$60\tau_{\text{knot}}$) for each knotted molecule. Note that hysteresis in the extension-Wi curves was not observed (see ESI†). We observe an abrupt increase in steady state extension
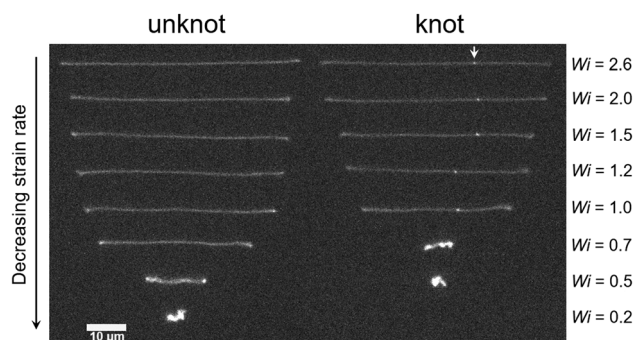


**Fig. 6** Images showing a molecule without a knot (left) and with a knot (right) stretched in planar elongational fields at strain rates from $\dot{\varepsilon} = 0.14$ s$^{-1}$ to $\dot{\varepsilon} = 1.75$ s$^{-1}$. Both molecules were observed at each strain rate for at least 2 minutes. The knotted molecule has a fractional knot size of 0.12 ± 0.04 at $\sim 30\%$ extension and a relaxation time of 1.27 ± 0.02 s ($\bar{\tau} = 0.82$). The reported Wi are determined relative to the unknot relaxation time. The white arrow indicates the presence of a knot along the chain.

of unknotted molecules around Wi = 0.5, in good agreement with previous experimental studies.[8,9,48] The knotted molecules are numbered in order of decreasing relaxation time (increasing knot size). The relaxation times and knot sizes of the knotted molecules are reported in Table S1 (see ESI†). As seen from Fig. 7a, at a given Wi, the knotted molecules always have smaller extensions compared to the unknotted molecules. Furthermore, the larger the knot on a molecule, the more shifted the extension-Wi curve becomes relative to the unknotted molecule. This signifies the importance of considering knotted molecules individually – a capability of single-molecule experiments – as the heterogeneity of knots can result in varying shifts of the coil–stretch transition.

To understand the shift in extension-Wi curves for knotted molecules, the change in relaxation time as a result of the occurrence of a knot needs to be considered. We can define an effective Weissenberg number

$$\text{Wi}_{\text{eff}} \equiv \dot{\varepsilon}\tau_{\text{knot}}. \tag{5}$$

It should also be recognized that knotted molecules are unable to attain the full chain contour length because of stored contour in the knot. To determine the maximum extension $L_{\text{max}}$ that the knotted molecule can achieve, we account for the stored contour in the knot and size of pixel window used to measure knot intensity at Wi > 2.5, as detailed in the ESI.† Fig. 7b displays the scaled steady-state extension as a function of Wi$_{\text{eff}}$. By defining Wi$_{\text{eff}}$ based on the knotted relaxation time and rescaling fractional extension by the maximum extension, we observe that the extension-Wi curves generally collapse onto the curve for the unknot, highlighting the importance of using the appropriate relaxation time to understand steady-state dynamics of knotted polymers.

Close inspection of Fig. 7b reveals poor overlap of the data at high extensions, with the data points for the knotted molecules vertically shifted to noticeably larger extensions compared to the unknotted molecules. This is perhaps to be expected, as the longest relaxation mode is dominant only at small chain extensions. Rescaling Wi by the longest relaxation time of each knotted molecule can approximately collapse the extension-Wi curves, but there is generally better overlap in the low extension compared to the high extension regime. At higher chain extensions, the contribution of higher order relaxation modes cannot be neglected and, as shown previously, the relaxation of a knotted chain is dependent on the knot size. Inspired by Narsimhan *et al.*,[40] we take into account the change in free chain contour at each strain rate when rescaling Wi. As discussed in Section 3.1, the knotted relaxation time based on Rouse scaling can be described as $\tau_{\text{rouse}} \propto (L_{\text{chain}} - L_{\text{knot}})^{1+2\nu}$. Hence, we have

$$\text{Wi}_{\text{rouse}} = \dot{\varepsilon}\tau_{\text{knot}} = \dot{\varepsilon}\tau_{\text{unknot}}\left(\frac{\tau_{\text{knot}}}{\tau_{\text{unknot}}}\right) = \text{Wi}\left(1 - \frac{L_{\text{knot}}}{L_{\text{chain}}}\right)^{1+2\nu}. \tag{6}$$

Similarly, based on Zimm scaling, we have

$$\text{Wi}_{\text{zimm}} = \text{Wi}\left(1 - \frac{L_{\text{knot}}}{L_{\text{chain}}}\right)^{3\nu}. \tag{7}$$
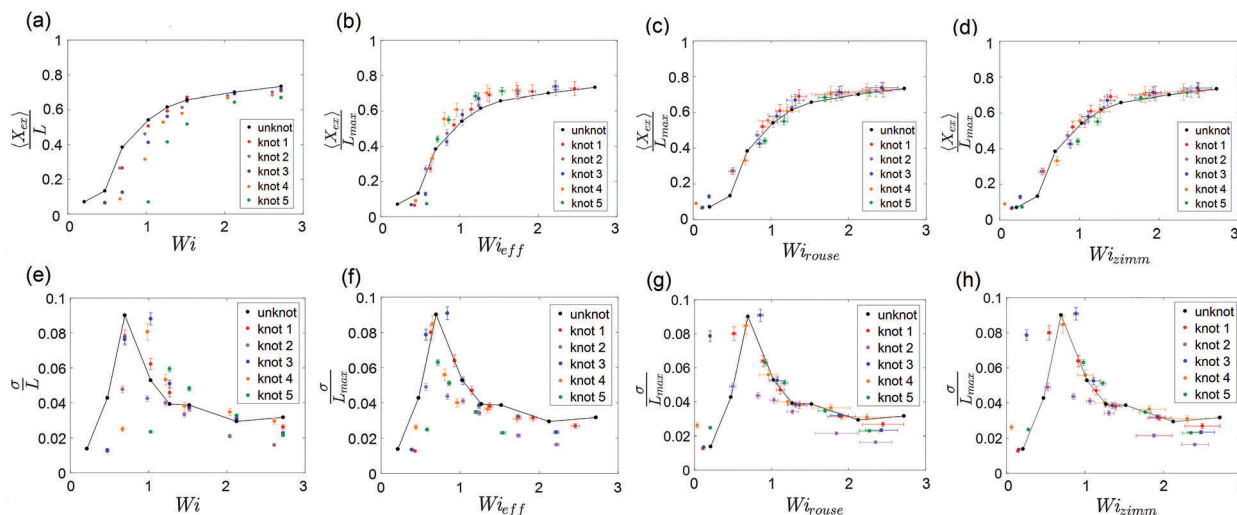
**Fig. 7** (a) Steady-state fractional extension as a function of $Wi = \dot{\varepsilon}\tau$ for unknotted and five different knotted molecules with varying knot sizes. (b–d) Scaled steady-state fractional extension as a function of $Wi_{eff} = \dot{\varepsilon}\tau_{knot}$, $Wi_{rouse} = Wi(1 - L_{knot}/L_{chain})^{1+2\nu}$ and $Wi_{zimm} = Wi(1 - L_{knot}/L_{chain})^{3\nu}$ for unknotted and the five knotted molecules presented in (a). (e) Standard deviation of steady-state fractional extension as a function of $Wi$ for unknotted and the five knotted molecules presented in (a). (f–h) Standard deviation of steady-state fractional extension as a function of $Wi_{eff}$, $Wi_{rouse}$ and $Wi_{zimm}$ for unknotted and the five knotted molecules presented in (a). The black lines are drawn to guide the eye. Error bars represent 95% confidence interval (see ESI† for calculation).

The knot sizes used to determine $Wi_{rouse}$ and $Wi_{zimm}$ for the knotted molecules at each strain rate are given in Table S2 (see ESI†). Fig. 7c and d show the scaled-steady state extension as a function of $Wi_{rouse}$ and $Wi_{zimm}$ respectively. For both cases, there is generally good collapse of the data onto the unknotted curve, especially in the high extension regime. It should be noted that rescaling $Wi$ by eqn (6) and (7) significantly shifts the data at low $Wi$, because the knot begins to take up a large proportion of the chain as the molecule approaches the coiled conformation. In an extended conformation, a knot is visibly apparent as a bright spot along chain. On the other hand, as the molecule approaches the coiled state, it is difficult to distinguish the arms of the chain from the knotted core, and the boundary between a knot and the chain arms is typically not well-defined. Therefore, the use of knot size in rescaling $Wi$ for experimental data may not be as appropriate in the low extension regime. The rescaling of extension-$Wi$ curves onto a master curve by defining an effective $Wi$ based on knot size has, however, been shown to be effective computationally.[40]

A unique feature of the coil–stretch transition is the critical slowdown in polymer dynamics toward steady state that is accompanied by enhanced molecule extension fluctuations.[11,62] The cause of this phenomenon is the large heterogeneity of polymer configurations corresponding to largely different chain extensions that are available close to the coil–stretch transition. As was done in previous studies,[11,48] we can examine the steady-state extension fluctuations by measuring the standard deviation of the steady-state fractional extensions. Fig. 7e shows the standard deviation of steady-state fractional extensions as a function of $Wi$ for the same unknotted and knotted molecules as in Fig. 7a–d. A peak in the standard deviation plot for unknotted molecules occurs at $Wi \approx 0.6$, in alignment with the location of significant increase in chain extension observed

in Fig. 7a and in good agreement with results reported in similar studies for T4 DNA.[11,48] The magnitude of the peak is also consistent with that measured by Gerashchenko and Steinberg[11] for T4 DNA in bulk elongational flow. Similar to the shift in extension-$Wi$ curves seen in Fig. 7a, the peaks in standard deviation plots for the knotted molecules are shifted to higher $Wi$, with the larger knots leading to larger shifts relative to the unknot.

We can rescale $Wi$ and standard deviation of steady-state extension in the standard deviation plots, as was performed for the extension-$Wi$ curves in Fig. 7b–d. The standard deviation of scaled steady-state extension as a function of $Wi_{eff}$, $Wi_{rouse}$ and $Wi_{zimm}$ are plotted in Fig. 7f–h. As seen from Fig. 7f, rescaling $Wi$ by the knotted relaxation time shifts the peaks in standard deviation for all knotted molecules to overlap with the peak corresponding to the unknotted molecules. The rescaling of $Wi$ taking into account a changing free chain contour (Fig. 7g and h) leads to a collapse of the standard deviation curves onto the unknotted curve at high strain rates. However, the data points surrounding the peaks at low strain rates are shifted such that peaks in the rescaled standard deviation plots no longer overlap. The difficulty in measuring a representative knot size at low chain extensions manifests itself in the incorrect scaling of $Wi$ near the coil–stretch transition. In the low extension regime, it is more suitable to rescale $Wi$ by the knotted relaxation time that characterizes the dominant relaxation mode at small chain extensions.

### 3.3 Changes in topology dynamically change the effective Wi and chain extension

Given that the occurrence of a knot changes the relaxation time of a molecule and shifts the coil–stretch transition, we expect the untying of a knot in elongational field near the coil–stretch
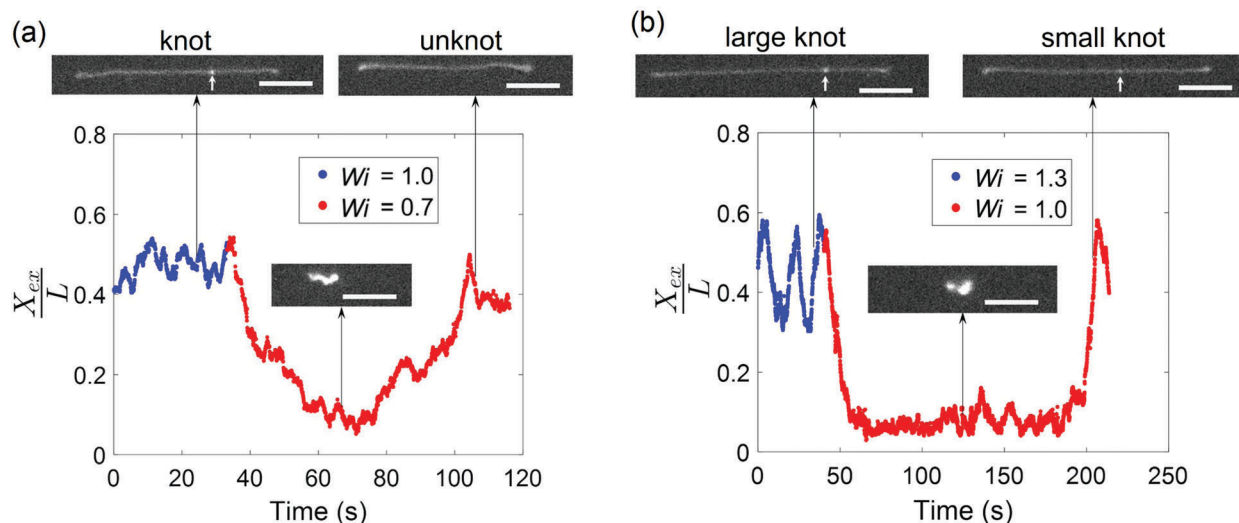
**Fig. 8** A change in topology near the coil–stretch transition leads to a change in effective Wi and chain conformation. (a) Fractional extension of a knotted molecule ($\tilde{L}$ = 0.08 $\pm$ 0.01 at Wi = 1.0) as it unties after Wi is decreased from 1.0 to 0.7. (b) Fractional extension of a knotted molecule ($\tilde{L}$ = 0.12 $\pm$ 0.02 at Wi = 1.3) as it unties into a smaller knot ($\tilde{L}$ = 0.04 $\pm$ 0.01 at Wi = 1.0) after Wi is decreased from 1.3 to 1.0. The white arrows indicate the presence of a knot along the chain. Scale bars represent 10 μm.

transition to change the effective Wi and, consequently, significantly impact the molecular conformation. Fig. 8 plots the fractional extension over time of two knotted molecules subjected to elongational fields as the applied strain rate is stepped down. As shown in Fig. 8a, the initially knotted molecule is stretched to around 50% extension at Wi = 1.0 ($\tilde{L}$ = 0.08 at Wi = 1.0) and undergoes the transition from a stretched to coiled state after Wi is decreased to 0.7. The molecule fluctuates around 10% extension for about 20 s, after which the molecule slowly stretches again and reveals the disappearance of the knot that was visibly apparent before. The presumed knot untying that occurred in the coiled configuration reversed the shift in coil–stretch transition caused by the knot's presence, such that the unknotted molecule is no longer below the coil–stretch transition and is hence elongated by the field.

A similar phenomenon is observed when a larger knot unties into a smaller knot. In Fig. 8b, a molecule containing a knot is initially stretched in an elongational field at Wi = 1.3 ($\tilde{L}$ = 0.12 at Wi = 1.3) and the large extension fluctuations suggest proximity to the molecule's coil–stretch transition. The molecule retracts into a coiled conformation after Wi is lowered to 1.0. It remains arrested in a compact state for about 150 s, or $\sim 100\tau_{\text{unknot}}$, before it is stretched by the field and a significantly less bright spot along the chain corresponding to a smaller knot ($\tilde{L}$ = 0.04 at Wi = 1.0) is observed. We note that the molecule undergoes extension fluctuations during the untying process. The long time required for the larger knot to partially untie in Fig. 8b relative to the time for a smaller knot to completely untie in Fig. 8a aligns with expectations that larger knots tend to be more complex topologically and hence cannot be untied as easily. This is in agreement with previous work demonstrating that molecules subjected to electric fields for longer durations undergo expansion processes characterized by longer time scales.[45] The vast changes in chain extension as knots untie

in the vicinity of the coil–stretch transition was also observed computationally by Narsimhan *et al.*[40] for various knot topologies. The presence and subsequent untying of a knot can lead to a molecule experiencing both a stretch–coil and coil–stretch transition at a fixed strain rate in elongational fields, highlighting the important effect that knots can have on the dynamics of polymers in steady-state fields.

## 4 Conclusion

In this work, we have systematically investigated the relaxation dynamics of knotted polymers and examined the steady-state behavior of knotted polymers in elongational fields. Experimental results show that the occurrence of a knot reduces the relaxation time of the molecule to an extent dependent on the knot size. Stored contour within the knot leads to a smaller amount of contour that is free to relax on the chain, which reduces the molecule's relaxation time. The decrease in relaxation time of knotted molecules can be qualitatively described by Rouse and Zimm scaling laws. The faster chain relaxation time due to a knot has consequences on the steady state dynamics of the knotted molecule in elongational fields. Specifically, a knot shifts the coil–stretch transition of the molecule such that the knotted polymer has a smaller extension than its unknotted counterpart at any given Wi. The extension-Wi curves and extension fluctuation plots for knotted molecules can be collapsed onto unknot curves by rescaling Wi with the measured knotted relaxation time in the low extension regime and a calculated relaxation time based on Rouse/Zimm scaling theories in the high extension regime. The change in chain relaxation time due to the presence of a knot and its effect on molecule dynamics in elongational fields is illustrated by the untying of a knot near the coil–stretch transition, which results

in the molecule experiencing at a fixed strain rate a stretch–coil transition with the knot and coil–stretch transition without the knot. From a broader perspective, given the ubiquity of knots in long polymers of both natural and synthetic origin, it is important to understand how the reduction of free chain contour due to the presence of a knot can influence the rheological properties of polymers. Looking forward, we hope that our work will motivate further experimental studies into the dynamics of knotted polymers, such as knotted molecule dynamics in confined environments and behavior in other flows or fields.

## Conflicts of interest

There are no conflicts to declare.

## Acknowledgements

## References

1 R. Pecora, *Science*, 1991, **251**, 893–898.
2 E. Y. Chan, N. M. Goncalves, R. A. Haeusler, A. J. Hatch, J. W. Larson, A. M. Maletta, G. R. Yantz, E. D. Carstea, M. Fuchs, G. G. Wong, S. R. Gullans and R. Gilmanshin, *Genome Res.*, 2004, **14**, 1137–1146.
3 K. Jo, D. M. Dhingra, T. Odijk, J. J. de Pablo, M. D. Graham, R. Runnheim, D. Forrest and D. C. Schwartz, *Proc. Natl. Acad. Sci. U. S. A.*, 2007, **104**, 2673–2678.
4 D. E. Smith, H. P. Babcock and S. Chu, *Science*, 1999, **283**, 1724–1727.
5 G. C. Randall, K. M. Schultz and P. S. Doyle, *Lab Chip*, 2006, **6**, 516–525.
6 W.-C. Liao, N. Watari, S. Wang, X. Hu, R. G. Larson and L. J. Lee, *Electrophoresis*, 2010, **31**, 2813–2821.
7 J. Tang and P. S. Doyle, *Appl. Phys. Lett.*, 2007, **90**, 224103.
8 T. T. Perkins, D. E. Smith and S. Chu, *Science*, 1997, **276**, 2016–2021.
9 D. E. Smith and S. Chu, *Science*, 1998, **281**, 1335–1340.
10 C. M. Schroeder, H. P. Babcock, E. S. G. Shaqfeh and S. Chu, *Science*, 2003, **301**, 1515–1519.
11 S. Gerashchenko and V. Steinberg, *Phys. Rev. E: Stat., Nonlinear, Soft Matter Phys.*, 2008, **78**, 040801.
12 A. Balducci, C.-C. Hsieh and P. S. Doyle, *Phys. Rev. Lett.*, 2007, **99**, 238102.
13 A. G. Balducci, J. Tang and P. S. Doyle, *Macromolecules*, 2008, **41**, 9914–9918.
14 P. G. de Gennes, *Science*, 1997, **276**, 1999–2000.
15 E. S. G. Shaqfeh, *J. Non-Newtonian Fluid Mech.*, 2005, **130**, 1–28.
16 Y. Li, K.-W. Hsiao, C. A. Brockman, D. Y. Yates, R. M. Robertson-Anderson, J. A. Kornfield, M. J. San Francisco,

C. M. Schroeder and G. B. McKenna, *Macromolecules*, 2015, **48**, 5997–6001.
17 R. M. Robertson, S. Laib and D. E. Smith, *Proc. Natl. Acad. Sci. U. S. A.*, 2006, **103**, 7310–7314.
18 D. J. Mai, A. B. Marciel, C. E. Sing and C. M. Schroeder, *ACS Macro Lett.*, 2015, **4**, 446–452.
19 C. B. Renner and P. S. Doyle, *Soft Matter*, 2015, **11**, 3105–3114.
20 A. R. Klotz, V. Narsimhan, B. W. Soh and P. S. Doyle, *Macromolecules*, 2017, **50**, 4074–4082.
21 D. W. Sumners and S. G. Whittington, *J. Phys. A: Math. Gen.*, 1988, **21**, 1689–1694.
22 M. D. Frank-Kamenetskii, A. V. Lukashin and A. V. Vologodskii, *Nature*, 1975, **258**, 398–402.
23 C. Micheletti, D. Marenduzzo, E. Orlandini and D. W. Sumners, *Biophys. J.*, 2008, **95**, 3591–3599.
24 L. Dai, J. R. C. van der Maarel and P. S. Doyle, *ACS Macro Lett.*, 2012, **1**, 732–736.
25 V. V. Rybenkov, N. R. Cozzarelli and A. V. Vologodskii, *Proc. Natl. Acad. Sci. U. S. A.*, 1993, **90**, 5307–5311.
26 S. Y. Shaw and J. C. Wang, *Science*, 1993, **260**, 533–536.
27 L. F. Liu, L. Perkocha, R. Calendar and J. C. Wang, *Proc. Natl. Acad. Sci. U. S. A.*, 1981, **78**, 5498–5502.
28 J. Arsuaga, M. Vázquez, S. Trigueros, D. W. Sumners and J. Roca, *Proc. Natl. Acad. Sci. U. S. A.*, 2002, **99**, 5373–5377.
29 O. Nureki, M. Shirouzu, K. Hashimoto, R. Ishitani, T. Terada, M. Tamakoshi, T. Oshima, M. Chijimatsu, K. Takio, D. G. Vassylyev, T. Shibata, Y. Inoue, S. Kuramitsu and S. Yokoyama, *Acta Crystallogr., Sect. D: Biol. Crystallogr.*, 2002, **58**, 1129–1137.
30 P. Virnau, L. A. Mirny and M. Kardar, *PLoS Comput. Biol.*, 2006, **2**, e122.
31 M. Schappacher and A. Deffieux, *Angew. Chem., Int. Ed.*, 2009, **48**, 5930–5933.
32 N. P. King, A. W. Jacobitz, M. R. Sawaya, L. Goldschmidt and T. O. Yeates, *Proc. Natl. Acad. Sci. U. S. A.*, 2010, **107**, 20732–20737.
33 A. Rosa, M. Di Ventra and C. Micheletti, *Phys. Rev. Lett.*, 2012, **109**, 118301.
34 V. Narsimhan, C. B. Renner and P. S. Doyle, *Soft Matter*, 2016, **12**, 5041–5049.
35 A. M. Saitta, P. D. Soper, E. Wasserman and M. L. Klein, *Nature*, 1999, **399**, 46–48.
36 S. R. Quake, *Phys. Rev. Lett.*, 1994, **73**, 3317–3320.
37 O. Farago, Y. Kantor and M. Kardar, *Europhys. Lett.*, 2002, **60**, 53–59.
38 C. Micheletti, D. Marenduzzo and E. Orlandini, *Phys. Rep.*, 2011, **504**, 1–73.
39 M. Caraglio, C. Micheletti and E. Orlandini, *Phys. Rev. Lett.*, 2015, **115**, 188301.
40 V. Narsimhan, A. R. Klotz and P. S. Doyle, *ACS Macro Lett.*, 2017, 1285–1289.
41 J.-F. Ayme, J. E. Beves, D. A. Leigh, R. T. McBurney, K. Rissanen and D. Schultz, *Nat. Chem.*, 2011, **4**, 15–20.
42 J.-F. Ayme, J. E. Beves, C. J. Campbell and D. A. Leigh, *Chem. Soc. Rev.*, 2013, **42**, 1700–1712.

43  Y. Harada, Y. Arai, R. Yasuda, K.-I. Akashi, H. Miyata, K. Kinosita and H. Itoh, *Nature*, 1999, **399**, 446–448.

44  X. R. Bao, H. J. Lee and S. R. Quake, *Phys. Rev. Lett.*, 2003, **91**, 265506.

45  J. Tang, N. Du and P. S. Doyle, *Proc. Natl. Acad. Sci. U. S. A.*, 2011, **108**, 16153–16158.

46  C. Zhou, W. W. Reisner, R. J. Staunton, A. Ashan, R. H. Austin and R. Riehn, *Phys. Rev. Lett.*, 2011, **106**, 248103.

47  G. C. Randall and P. S. Doyle, *Macromolecules*, 2005, **38**, 2410–2418.

48  J. Tang, D. W. Trahan and P. S. Doyle, *Macromolecules*, 2010, **43**, 3081–3089.

49  A. C. Klepinger, M. K. Greenier and S. L. Levy, *Macromolecules*, 2015, **48**, 9007–9014.

50  G. C. Randall and P. S. Doyle, *Proc. Natl. Acad. Sci. U. S. A.*, 2005, **102**, 10813–10818.

51  B. Kundukad, J. Yan and P. S. Doyle, *Soft Matter*, 2014, **10**, 9721–9728.

52  A. Y. Grosberg and Y. Rabin, *Phys. Rev. Lett.*, 2007, **99**, 217801.

53  L. Dai, C. B. Renner and P. S. Doyle, *Macromolecules*, 2014, **47**, 6135–6140.

54  T. T. Perkins, S. R. Quake, D. E. Smith and S. Chu, *Science*, 1994, **264**, 822–826.

55  N. Clisby, *Phys. Rev. Lett.*, 2010, **104**, 055702.

56  P. E. Rouse, Jr., *J. Chem. Phys.*, 1953, **21**, 1272–1280.

57  B. H. Zimm, *J. Chem. Phys.*, 1956, **24**, 269–278.

58  A. Balducci, P. Mao, J. Han and P. S. Doyle, *Macromolecules*, 2006, **39**, 6273–6281.

59  J. J. Jones, J. R. C. van der Maarel and P. S. Doyle, *Phys. Rev. Lett.*, 2013, **110**, 068101.

60  P. G. de Gennes, *J. Chem. Phys.*, 1974, **60**, 5030–5042.

61  R. G. Larson and J. J. Magda, *Macromolecules*, 1989, **22**, 3004–3010.

62  A. Celani, A. Puliafito and D. Vincenzi, *Phys. Rev. Lett.*, 2006, **97**, 118301.